

**CONCEPTUAL DESIGN AND DYNAMICAL
ANALYSIS OF AEROSTAT SYSTEM**

KHURRUM MAHMOOD

UNIVERSITI SAINS MALAYSIA

2020

**CONCEPTUAL DESIGN AND DYNAMICAL ANALYSIS OF AEROSTAT
SYSTEM**

by

KHURRUM MAHMOOD

**Thesis submitted in fulfillment of the
requirements for the degree of
Master of Science**

November 2020

ACKNOWLEDGEMENT

First and foremost, praises and thanks to Allah Almighty, for His help and blessings in my entire life and during my research work that has made me able to complete my thesis successfully.

I would like to express my sincere gratitude to my supervisor Dr. Norilmi Amilia Ismail to provide me with the opportunity to work in Space Systems Lab of School of Aerospace Engineering. Her dynamism, vision, sincerity and motivation have deeply inspired me. Her broad knowledge and experience in the field of Aerospace Engineering has helped me to conduct research in my Master's studies. It was a great privilege and honor to work and study under her guidance. I offer my sincere appreciation to my co-supervisor, Dr. Nurulasikin Mohd Suhadis for her exemplary guidance throughout the project.

I am extremely grateful to my parents for their love, prayers, caring and sacrifices for educating and preparing me for my future. I would express special gratitude to my father; completing this milestone would be a sense of great achievement for him if he would have been in this world today. I would like to thank my wife Erum Ashraf, to provide immense support during my studies. My special thanks goes to my brother Major Khawir Mahmood who kept me motivated to pursue my higher education. Last but not least I would like to thank Dr. Mateen ud Din Qazi who trained me with dynamic simulation tools and has been a source of inspiration since the start of my professional career in Center of Excellence in Applied Sciences Pakistan. Finally, my thanks go to all the people who have supported me to complete the research work directly or indirectly.

TABLE OF CONTENTS

ACKNOWLEDGEMENT	ii
TABLE OF CONTENTS	iii
LIST OF TABLES	ix
LIST OF FIGURES	xi
LIST OF SYMBOLS	xv
LIST OF ABBREVIATIONS	xix
ABSTRAK	xxi
ABSTRACT	xxiv
CHAPTER 1 INTRODUCTION	1
1.1 Research Background	1
1.2 Problem Statement	4
1.3 Research Objectives	4
1.4 Research Scope	4
1.5 Thesis Outline	5
CHAPTER 2 LITERATURE REVIEW	7
2.1 Introduction to Tethered Aerostat Systems	7
2.2 Subsystems of TAS	7
2.2.1 Aerostat	8
2.2.1(a) Aerostat Hull Shapes	9
2.2.1(b) Aerostat Hull Shape Comparison	11
2.2.1(c) Ballonet	13

2.2.1(d)	Aerostat Hull Material	14
2.2.2	Payload	15
2.2.3	Tether	16
2.2.4	Winch	16
2.2.5	Mooring Station	18
2.3	TAS Categorization	19
2.3.1	Tactical Aerostats	20
2.3.2	Operational Aerostat	21
2.3.3	Strategic Aerostats	21
2.4	TAS Design Process	21
2.4.1	Input Data	22
2.4.1(a)	Payload Specifications	22
2.4.1(b)	Material Properties	23
2.4.1(c)	LTA Gas Properties	23
2.4.2	Atmospheric Calculations	23
2.4.3	Hull Parameters	24
2.4.3(a)	Envelope Shape Selection	24
2.4.3(b)	Hull Volume	25
2.4.3(c)	Gross Lift	25
2.4.4	Tether Profile	25
2.4.5	Fin Sizing	26
2.4.6	Weight Calculation	26
2.5	TAS Design Optimization Studies	27
2.5.1	Optimization for drag coefficient reduction of Hull	27
2.5.2	Multi-disciplinary design optimization of hull	28

2.6	TAS Dynamical Analysis	29
2.7	Research Gap	31
CHAPTER 3 RESEARCH METHODOLOGY		33
3.1	Baseline Configuration Design	33
3.1.1	User Requirement	35
3.1.2	Preliminary Design Parameters	36
3.1.2(a)	Atmospheric Properties	36
3.1.2(b)	Hull and Fins Material Properties	37
3.1.2(c)	Tether Properties	38
3.1.2(d)	LTA Gas	38
3.1.3	Sizing and Mass Estimation	38
3.1.3(a)	Hull Sizing	38
3.1.3(b)	Fin Sizing	40
3.1.3(c)	Mass Estimation	42
3.1.3(d)	Buoyant Force	43
3.1.4	Aerodynamic Forces	44
3.1.4(a)	Aerodynamic Forces on Hull	45
3.1.4(b)	Aerodynamic Forces on Fins	47
3.1.5	Static Stability	48
3.1.6	Performance Analysis	50
3.1.7	Design Algorithm	51
3.1.8	Validation of MATLAB® Design Algorithm	52
3.2	Design Optimization	53
3.2.1	Design Variables	54

3.2.1(a)	Hull fineness ratio	54
3.2.1(b)	Fin Area	54
3.2.1(c)	Fin Location	55
3.2.2	Sensitivity Analysis	56
3.2.3	Objective Function	57
3.2.4	Optimization Algorithms	58
3.3	GUI Development	59
3.4	Dynamic Simulation Model	63
3.4.1	Aerostat Model	66
3.4.2	Tether Model	59
3.4.3	Wind Model	68
CHAPTER 4 RESULTS AND DISCUSSION		70
4.1	Baseline Configuration	70
4.1.1	Input Parameters	70
4.1.2	Geometric Parameters of Baseline Configuration	71
4.1.3	Mass breakdown of Baseline Configuration	72
4.1.4	Performance parameters of Baseline Configuration	72
4.1.5	Performance plots of Baseline Configuration	72
4.2	Sensitivity Analysis	75
4.2.1	Fineness Ratio	75
4.2.2	Fin Area	76
4.2.3	Fin Location	78
4.3	Optimization	81
4.3.1	Design variable bounds	81

4.3.2	Objective Function	82
4.3.3	Optimization Results	82
4.3.3(a)	<i>fmincon</i>	83
4.3.3(b)	Surrogate Optimization	84
4.3.3(c)	Particle Swarm Optimization	85
4.3.3(d)	Results Comparison	86
4.4	Optimized Configuration	87
4.4.1	Geometric Parameters	87
4.4.2	Mass Breakdown	87
4.4.3	Performance Parameters	88
4.4.4	Comparison of configurations size	88
4.4.5	Comparison of configuration performance	89
4.5	Aerostat Design App (GUI)	92
4.5.1	Test Case 1: Results for different values of Payload Mass	94
4.5.2	Test Case 2: Results for different values of Altitude	96
4.6	Dynamic Simulation Results	99
4.6.1	Tether Profile	99
4.6.2	Aerostat response to varying wind speed	100
4.6.3	Aerostat response to gust wind	102
4.6.4	Aerostat response to turbulent wind	103
CHAPTER 5 CONCLUSION		105
5.1	Research Summary	105
5.2	Future Work	107
REFERENCES		108

APPENDICES

115

Appendix A: Atmospheric Parameters

Appendix B: Tether Properties

Appendix C: Aerodynamic Apparent Mass Coefficients

Appendix D: Hull Shape Integrals

Appendix E: Solidworks Model for MATLAB Algorithm Validation

Aerostat Mass and Center of Gravity

Appendix F: GUI Callback function

Appendix G: Added Mass Matrix

Appendix H: Helium Gas Cost

LIST OF PUBLICATIONS

LIST OF TABLES

Table 2.1	Aerostat hull shapes comparison (Mahmood, Ismail and Suhadis, 2020)	11
Table 2.2	Hull Shape Parameters for calculating Blow-by	12
Table 2.3	Tactical, Operational and Strategic Class Aerostats (SAVER, 2013)	20
Table 2.4	User Requirement	22
Table 2.5	LTA gas properties	23
Table 3.1	Fabric material GSM	37
Table 3.2	Hull Fineness Ratios	40
Table 3.3	Fin Parameters using statistical data	40
Table 3.4	Validation of Geometric Parameters	52
Table 3.5	Validation of Inertial Parameters	53
Table 4.1	Requirement Specification	70
Table 4.2	Baseline Configuration Mass Breakdown	72
Table 4.3	Baseline Configuration Results	72
Table 4.4	Sensitivity analysis results for hull fineness ratio	76
Table 4.5	Sensitivity analysis results for fin area increase	77
Table 4.6	Sensitivity analysis results for change in fin location	81
Table 4.7	Lower and upper bound of design variables	82
Table 4.8	<i>fmincon</i> results	83
Table 4.9	<i>fmincon</i> results using <i>Global Search</i>	84
Table 4.10	Surrogate Optimization results	84
Table 4.11	PSO results	85
Table 4.12	Optimization Results	86
Table 4.13	Optimized Configuration Mass Breakdown	88

Table 4.14	Optimized Configuration Results	88
Table 4.15	Input Values for Test Cases	93

LIST OF FIGURES

Figure 1.1	Aerial Vehicle Categorization	1
Figure 1.2	System Architecture for LAP System for Communication	3
Figure 2.1	Aerostat Subsystems	8
Figure 2.2	Skystar 220 Spherical Aerostat (RT, no date)	9
Figure 2.3	Helikite (Allsopp Helikites Ltd, no date)	10
Figure 2.4	Streamlined Shape Aerostat (TCOM, 2018)	11
Figure 2.5	Blow-by comparison of different hull shapes	13
Figure 2.6	Ballonet (TCOM, 2018)	14
Figure 2.7	Aerostat Hull Material Layers	15
Figure 2.8	Aerostat Payloads	16
Figure 2.9	Live Tether for Aerostat (Linden Photonics, 2020)	16
Figure 2.10	TAS Winch System	17
Figure 2.11	Winch (Thern, 2019)	17
Figure 2.12	Mooring Station of Smaller Aerostat (SkySentry, no date)	18
Figure 2.13	Mooring Station of Larger Aerostats (SAVER, 2013)	18
Figure 2.14	Mobile Mooring Station	19
Figure 2.15	Aerostat Design Process	22
Figure 2.16	Standard Streamlined Shapes (Alam and Pant, 2017)	24
Figure 3.1	Outline for Design and Analysis of TAS	33
Figure 3.2	Design Process	34
Figure 3.3	Average Hourly Wind Speed (Mersing, Jan 2009)	36
Figure 3.4	NPL Shape	39

Figure 3.5	Aerostat Fin Parameters	41
Figure 3.6	Fin Cross-section Volume and Curve	41
Figure 3.7	Aerodynamic Forces on Hull	45
Figure 3.8	Fin Center of Pressure	47
Figure 3.9	Forces acting on Aerostat at Equilibrium Condition	49
Figure 3.10	Formulae to obtain Tether Profile (Rajini, Pant and Sudhakar, 2010)	50
Figure 3.11	Design Algorithm Operation	52
Figure 3.12	Layout of Sensitivity Analysis	56
Figure 3.13	Layout of Optimization Process	57
Figure 3.14	Tethered Aerostat Schematic	60
Figure 3.15	Simscape Tether Element Model	61
Figure 3.16	MATLAB® App Designer Layout	62
Figure 3.17	GUI Aerostat Design	63
Figure 3.18	Reference Coordinate System	64
Figure 3.19	Schematic diagram of TAS simulation model	65
Figure 3.20	Simscape TAS model	65
Figure 3.21	Forces on Aerostat	66
Figure 3.22	Simscape aerostat model	67
Figure 3.23	Aerostat body block	67
Figure 3.24	Simscape varying wind model	68
Figure 3.25	Simscape gust wind model	69
Figure 3.26	Simscape turbulent wind model	69
Figure 4.1	Baseline Configuration Geometry Parameters	71
Figure 4.2	Blow-by with Wind Speed (Baseline Configuration)	73
Figure 4.3	Equilibrium AoA with Wind Speed (Baseline Configuration)	73

Figure 4.4	Dynamic Lift with Wind Speed (Baseline Configuration)	74
Figure 4.5	Tether Tension with Wind Speed (Baseline Configuration)	74
Figure 4.6	Moment coefficient with AoA (Baseline Configuration)	75
Figure 4.7	Volumetric drag coefficient versus AoA for different Hull FR	76
Figure 4.8	Dynamic Lift versus Fin Area Increase	77
Figure 4.9	Equilibrium AoA vs Wind Speed for different Fin Areas	78
Figure 4.10	Fin at different locations	79
Figure 4.11	Equilibrium AoA vs Wind Speed for different Fin Locations	80
Figure 4.12	Dynamic Lift versus Fin Location	80
Figure 4.13	Surrogate Optimization	85
Figure 4.14	PSO Optimization	86
Figure 4.15	Optimized Configuration Geometry Parameters	87
Figure 4.16	Optimized Configuration Improvement	89
Figure 4.17	Comparison of Configurations	89
Figure 4.18	Dynamic Lift with Wind Speed (Comparison)	90
Figure 4.19	Blow-by with Wind Speed (comparison)	90
Figure 4.20	Equilibrium AoA with Wind Speed (Comparison)	91
Figure 4.21	Tether Tension with Wind Speed (Comparison)	91
Figure 4.22	Moment coefficient with AoA (Comparison)	92
Figure 4.23	Aerostat Design App	93
Figure 4.24	Blow-by Test Case 1 (10 kg Payload)	94
Figure 4.25	Equilibrium AoA Test Case 1 (10 kg Payload)	94
Figure 4.26	Tether Profile Test Case 1 (10 kg Payload)	95

Figure 4.27	Blow-by Test Case 1 (30 kg Payload)	95
Figure 4.28	Equilibrium AoA Test Case 1 (30 kg Payload)	96
Figure 4.29	Tether Profile Test Case 1 (30 kg Payload)	96
Figure 4.30	Blow-by Test Case 2 (100 m Altitude)	97
Figure 4.31	Equilibrium AoA Test Case 2 (100 m Altitude)	97
Figure 4.32	Tether Profile Test Case 2 (100 m Altitude)	97
Figure 4.33	Blow-by Test Case 2 (500 m Altitude)	98
Figure 4.34	Equilibrium AoA Test Case 2 (500 m Altitude)	98
Figure 4.35	Tether Profile Test Case 2 (500 m Altitude)	99
Figure 4.36	Tether Profile	99
Figure 4.37	Aerostat response to varying winds	100
Figure 4.38	Tension in viscoelastic element	101
Figure 4.39	Aerostat response to gust wind	102
Figure 4.40	Tension in viscoelastic element due to gust wind	103
Figure 4.41	Aerostat response to turbulent wind	104

LIST OF SYMBOLS

α	Angle of attack
a_1	Front ellipse semi major axis
a_2	Rear ellipse semi major axis
α_{eq}	Equilibrium angle of attack
A_f	Fin axial aerodynamic force
A_h	Hull axial aerodynamic force
AR	Aspect Ratio
b	Hull radius
C	Confluence point
C_D	Fin drag coefficient
C_{D0}	Fin zero lift drag coefficient
C_{DV}	Volumetric drag coefficient
$(C_{dh})_o$	Hull axial drag coefficient
$(C_{dc})_h$	Cross flow drag coefficient
C_h	Hull centroid
C_f	Fin centroid
C_L	Fin lift coefficient
C_{La}	3D lift coefficient slope
C_{la}	Airfoil lift coefficient slope
C_m	Moment coefficient
C_{ma}	Moment coefficient slope
Δl_f	Fin position percentage of hull length
ΔS_f	Percentage increase in fin area

d	Diameter
D_{fin}	Fin drag
dW	Weight of tether segment
dD	Drag of tether segment
e	Oswald's efficiency factor
ζ	Axial distance from hull nose
f	Hull fineness ratio
F_B	Buoyancy force
F_{RA}	Fin reference area
λ	Fin sweep angle
g	Gravity
H_{RA}	Hull reference area
I_1, J_1, I_3, J_2	Hull shape integrals
k	Purity of LTA gas
k_3-k_1	Apparent mass coefficients
l	Hull length
l_f	Fin location
l_h	Distance of fin from nose
l_t	Tether length
L_{dyn}	Dynamic lift
L_f	Free lift
L_{fin}	Fin lift
m_a	Aerostat mass
m_{fin}	Fin mass
m_{hull}	Hull mass

m_p	Payload mass
m_t	Tether mass
m_{Total}	Total mass
M_A	Hull aerodynamic moment
M_{Added}	Added mass matrix
n	Number of moles
η_k	Fin efficiency factor
n_s	Number of segments of tether
N_f	Fin normal aerodynamic force
N_h	Hull normal aerodynamic force
P	Hull pressure
q_o	Dynamic pressure
ρ_f	Density of fin fabric material
ρ_{LTA}	LTA gas density
ρ_t	Density of tether material
ρ_{gas}	LTA gas density at atmospheric pressure
ρ_{air}	Air density
ρ_{total}	LTA gas density at pressurized hull
r	Hull radius
RC	Root chord
Re	Reynolds number
S_f	Fin surface area
S_h	Hull surface area
S_p	Fin span
θ	Tether angle

θ_c	Tether angle at confluence point
θ_{eq}	Equilibrium angle of attack
θ_v	Wind angle
t	Time
T	Tether tension force
T_a	Air temperature
T_x	Tether tension x-component
T_z	Tether tension z-component
TC	Tip chord
v	Wind speed
v_o	Wind speed at reference height
V	Hull volume
V_a	Aerostat volume
V_f	Fin volume
V_x	Aerostat velocity along x-axis
V_z	Aerostat velocity along z-axis
W	Aerostat weight
x	Blow-by
X_c	Confluence point location
X_{CP1}	Center of pressure of hull
X_{CP2}	Center of pressure of fin
z	Height
z_o	Reference height
Z_c	Confluence point location

LIST OF ABBREVIATIONS

AoA	Angle of Attack
BL	Baseline
CAD	Computer Aided Design
CB	Center of Buoyancy
CFD	Computational Fluid Dynamics
CG	Center of Gravity
CP	Center of Pressure
CPSO	Constrained Particle Swarm Optimization
DoF	Degrees of Freedom
EO/IR	Electro-Optical/Infra-Red
GSM	Grams per Square Meter
GUI	Graphic User Interface
HALE	High Altitude Long Endurance
HAP	High Altitude Platform
HTA	Heavier Than Air
ISA	International Standard Atmosphere
LAP	Low Altitude Platform
LTA	Lighter Than Air
MDO	Multidisciplinary Design Optimization
NACA	National Advisory Committee for Aeronautics
OPT	Optimized
PSL	Percentage Static Lift
PSO	Particle Swarm Optimization

PU	Poly Urethane
PVC	Poly Vinyl chloride
RRH	Remote Radio Head
SIGINT	Signal Intelligence
SO	Surrogate Optimization
TAS	Tethered Aerostat System
UAVs	Unmanned Aerial Vehicles
UV	Ultraviolet
VCM	Variable Complexity Modeling

REKABENTUK KONSEP DAN ANALISIS DINAMIK SISTEM AEROSTAT

ABSTRAK

Aerostat tertambat adalah sistem udara yang cekap untuk pelbagai kegunaan. Sistem Taktikal Aerostat tertambat dianggap sebagai sistem boleh digunakan sebagai sistem maklumbalas kecemasan dalam memulihkan sistem komunikasi selepas berlaku bencana alam. Sistem ini beroperasi tanpa sistem pendorong dan kawalan membuatnya mudah untuk dipasang. Namun, sistem ini harus tetap stabil dengan kehadiran angin atmosfera dan boleh meminimumkan pergeseran yang disebabkan oleh angin dan ini dinamakan tiupan pindah. Penyelidikan ini mengemukakan konfigurasi aerostat yang baharu untuk digunakan sebagai sistem taktikal yang mana nisbah kehalusan lambung dan sirip direkabentuk untuk menghasilkan daya angkat aerodinamik untuk meminimumkan tiupan pindah. Rekabentuk yang dioptimumkan menggunakan pendekatan ini dapat beroperasi dengan pdaya angkat statik yang lebih rendah dan dapat mengurangkan saiz aerostat, menjadikannya lebih padat dan menjimatkan kos.

Pendekatan rekabentuk aerostat yang digunakan merangkumi aerostatik, anggaran berat, aerodinamik, kestabilan statik dan tiupan pindah, digunakan untuk mengembangkan algoritma reka bentuk dalam MATLAB®. Reka bentuk dan pengoptimuman aerostat dilakukan dengan mengambil jisim muatan 10 kg dan ketinggian operasi menjadi 300 meter. Konfigurasi rekabentuk asas untuk misi yang diinginkan telah diperoleh menggunakan kod rekabentuk di mana nilai statistik pemboleh ubah reka bentuk yang dipilih merangkumi nisbah kehalusan lambung aerostat, luas sirip dan kedudukan sirip aerostat yang digunakan. Analisis kepekaan

telah dilakukan untuk menentukan pengaruh pemboleh ubah reka bentuk pada jisim aerostat dan tiupan pindah. Aerostat dioptimumkan dengan menetapkan pengurangan jisim sebagai fungsi objektif, mengambil batas bawah dan atas pemboleh ubah reka bentuk dan had tiupan sebagai kekangan. Keputusan menunjukkan bahawa konfigurasi yang dioptimumkan mempunyai isipadu lambung yang lebih kecil yang boleh mengurangkan jisim sistem. Sirip aerostat yang dioptimumkan pula menghasilkan pengangkatan aerodinamik untuk beroperasi dalam had tiupan pindah dan memberikan kestabilan putaran. Sirip aerostat yang dioptimumkan menghasilkan daya angkat aerodinamik untuk beroperasi dalam had tiupan pindah dan memberikan kestabilan putaran. Konfigurasi aerostat yang dioptimumkan menunjukkan pengurangan isipadu daripada 170 m^3 kepada 120 m^3 , penurunan jisim daripada 90.65 kg kepada 71.6 kg . Pengurangan isipadu konfigurasi yang dioptimumkan telah mengurangkan kos Helium sehingga RM 7700.00.

Antara muka pengguna grafik telah dibangunkan menggunakan pembangun aplikasi MATLAB® untuk kegunaan reka bentuk. Algoritma reka bentuk dihubungkan dengan aplikasi antara muka pengguna grafik dan jisim muatan, ketinggian operasi dan sifat bahan adalah parameter input. Parameter geometri, jisim dan prestasi untuk reka bentuk konsep diperoleh dari aplikasi reka bentuk.

Analisis dinamik aerostat dilakukan dengan membangunkan model simulasi yang mempunyai kebebasan tiga darjah. Simscape Multibody™, aplikasi lanjutan dari MATLAB® / Simulink yang menggunakan teknik pemodelan berasaskan blok digunakan untuk mengembangkan model kebebasan darjah tiga. Aerostat dimodelkan sebagai badan kaku tunggal sementara penambat telah dimodelkan sebagai urutan elemen yang disambungkan pada nod melalui tahap kebebasan revolut. Aerostat disimulasikan untuk keadaan angin normal, hembusan angin dan angin bergelora

yang berbeza-beza untuk menganalisis kestabilan membujur. Hasil simulasi menunjukkan bahawa konfigurasi aerostat yang dioptimumkan mempunyai kestabilan dinamik membujur untuk setiap senario angin yang berbeza. Aerostat dilihat mencapai keadaan stabil dengan perubahan anggul dalam lingkungan ± 3 darjah setelah berada dalam keadaan angin yang bertiup tidak sekata atau angin bertiup perlahan dalam masa 40 saat . Dalam keadaan angin bergelora berintensiti tinggi, halaju mendatar aerostat berubah-ubah ± 1.2 m/s, dan halaju menegak berubah dalam lingkungan ± 0.2 m/s dan perubahan angul dalam ± 3.5 darjah.

CONCEPTUAL DESIGN AND DYNAMICAL ANALYSIS OF AEROSTAT SYSTEM

ABSTRACT

Tethered aerostats are an efficient aerial system to be used for different applications. Tactical category of tethered aerostat systems is deemed as an emergency respondent system in restoration of communication aftermath a natural disaster. They operate without a propulsive and control system making it easy to deploy. However, it has to remain stable in the presence of atmospheric winds and minimize the drift due to wind called blow-by. This research thesis presents a novel streamlined aerostat configuration to be used as a tactical system in which the hull fineness ratio and fins are designed to generate aerodynamic lift to minimize the blow-by. The optimized design obtained using this approach can operate with lesser static lift that reduces the aerostat size making it cost effective and compact.

The aerostat design approach that includes aerostatics, mass estimation, aerodynamics, static stability and blow-by is used to develop a design algorithm in MATLAB®. The design and optimization of the aerostat is carried out by taking payload mass of 10 kg and operating altitude to be 300 meter. The baseline configuration for the desired mission has been obtained using a design algorithm. The statistical values of the selected design variables that include hull fineness ratio, fin area and fin position of the existing aerostat are used to obtain the baseline configuration. The sensitivity analysis has been carried out to determine the effect of design variables on the aerostat mass and blow-by. The aerostat is optimized by setting minimization of mass as the objective function, taking lower and upper bounds of the

design variables and blow-by limit as the constraint. The results show that the optimized configuration has a smaller hull volume that reduces the mass of the system. The fins of the optimized aerostat generate aerodynamic lift to operate within the blow-by limits along with providing rotational stability. The optimized configuration of the aerostat shows a reduction in volume to 120 m^3 from 170 m^3 , reduction in mass to 71.6 kg from 90.65 kg. The reduction in volume of optimized configuration reduces the LTA gas Helium cost up to USD1925 (RM7700).

A graphic user interface has been developed using MATLAB® app developer for design application. The design code is linked with the graphic user interface of the design app in which the payload mass, operating altitude and material properties are the input parameters. The geometric, mass and performance parameters for the conceptual design are obtained from the design app.

The dynamical analysis of the aerostat is conducted by developing a three degree of freedom simulation model. Simscape Multibody™, an extension of MATLAB®/Simulink that employs a block-based modelling technique is used to develop the three degrees of freedom model. The aerostat is modeled as a single rigid body while the tether has been modeled as a sequence of elements connected at nodes through a revolute degree of freedom. The aerostat is simulated for varying winds, gusts and turbulent wind to analyze the longitudinal stability. The results show that the optimized aerostat configuration has longitudinal dynamic stability for the different wind scenarios. The aerostat attains steady state after encountering a varying wind or gust wind within 40 secs with $\pm 3^\circ$ fluctuations in pitch. For high intensity turbulent wind, the aerostat fluctuates with $\pm 1.2 \text{ m/s}$ horizontal velocity, $\pm 0.2 \text{ m/s}$ vertical velocity and $\pm 3.5^\circ$ pitch.

CHAPTER 1

INTRODUCTION

1.1 Research Background

The aerial vehicles can be categorized primarily as heavier than air (HTA) and lighter than air (LTA) vehicles. The former generates the lift force is generated through the dynamic pressure of air to float in the air. The latter utilizes the buoyancy force of helium or hydrogen gas inside its envelope to float in the air. The flowchart depicting the categorization of aerial vehicles is given in Figure 1.1 (Rapid Reaction Technology Office Washington, 2012).

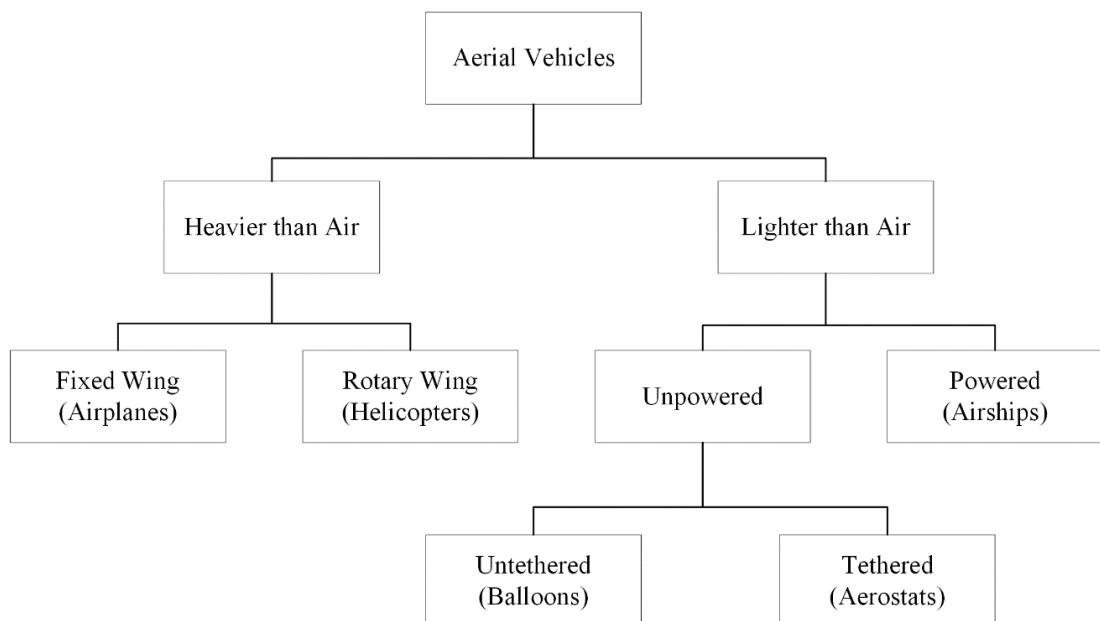


Figure 1.1 Aerial Vehicle Categorization

Tethered aerostat systems (TAS) are a class of LTA vehicles that are tied to the ground via a tether that maintains its position and provides power to the onboard equipment from the ground. Like airships, TAS is the most efficient systems as they

depend entirely on the LTA gas buoyancy to float in the air and can operate for long durations. The operating altitude of the TAS depends on the size of the aerostat. They can carry payload containing communication equipment and digital cameras or Electro-Optical and Infra-red (EO/IR) Sensors. Modern TAS are used for a variety of applications that includes surveillance, wireless communication, emergency relief operations, agricultural field monitoring and protection, atmospheric data recording, electric power generation, aerial photography, and space exploration (Young-heon *et al.*, 2015; Chandrasekharan *et al.*, 2016; Dusane *et al.*, 2017; Ghosh, Guha and Duttagupta, 2017; Dexheimer, 2018; Saleem and Kim, 2018).

The tactical category of TAS having a low altitude of operation is deemed as an efficient solution to provide communication to remote and rural areas (Gawande *et al.*, 2007). In addition to rural areas it is deemed as a best candidate solution to provide communication access to disaster affected areas. Natural disasters like earthquake and tsunami cause damage to the terrestrial communication infrastructure that disrupts communication. Disaster relief operations are challenging to perform in the absence of communication links. The relief operation consists of providing instructions to the people of affected zones, collect data of people that require rescue aid and interdepartmental communication of the relief teams (Gomez *et al.*, 2013; Almalki and Angelides, 2019). The restoration of communication by fixing the terrestrial infrastructure is a time consuming and costly process. A cost-effective stationary low altitude platform (LAP) communication system that consists of aerial platforms is a potential solution that can quickly restore the communication to the affected areas (Chandrasekharan *et al.*, 2016). Tactical TAS can act as an emergency respondent system by replacing the broken terrestrial communication links. It can be deployed in

a very short time with minimum manpower through a vehicle, boat or stationary station (TCOM, 2018).

A layout of the system architecture of a TAS replacing a terrestrial tower and restoring communication is depicted in Figure 1.2. The mobile base station is present at the ground vehicle that is connected to the onboard payload electronics including antennas carried by the aerostat through fiber optic cable inside the tether. The antenna receives and transmits the signals in the cellular network to customer cellular devices and connects them to the network operator through the base station.

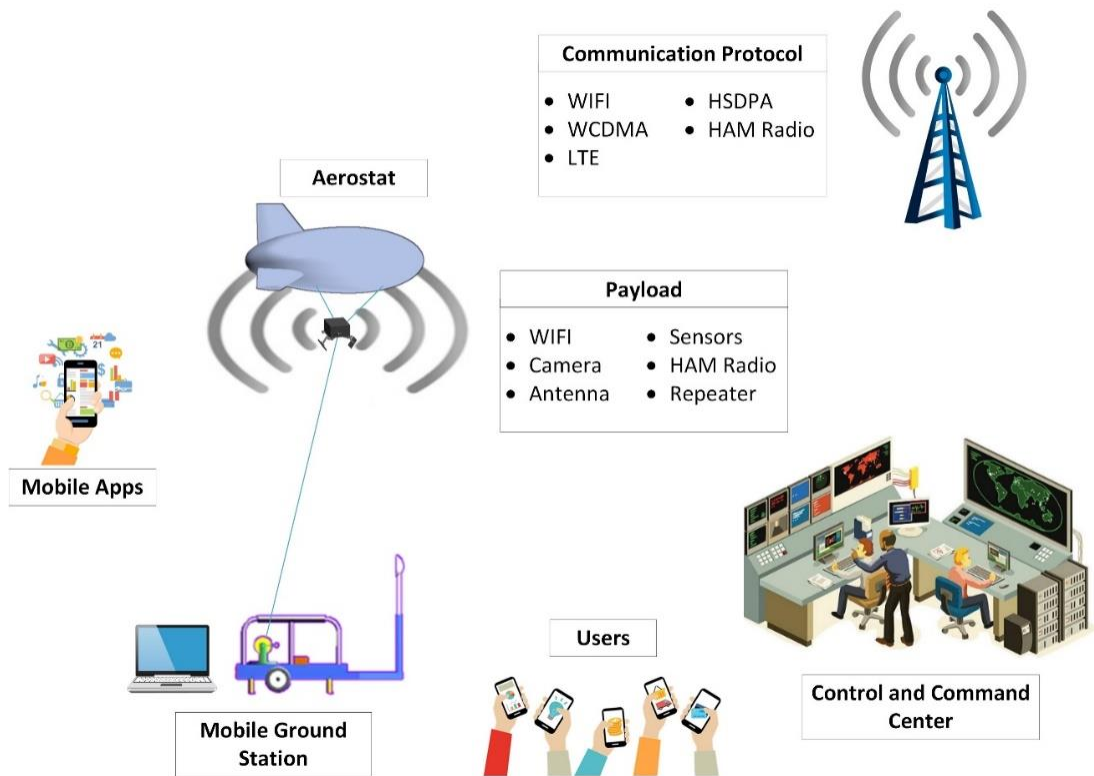


Figure 1.2 System Architecture for LAP System for Communication

TAS can be deployed readily by the minimum crew and are highly portable. However, a TAS has no power source and active control to maintain its position when acted upon by atmospheric winds and causes it to displace from its mean position

called blow-by (Ram and Pant, 2010; Kumar, Sati and Ghosh, 2016). For the effective functionality of the payload, it is required that the TAS operates remaining as static as possible (De Azevedo, Góes and Azinheira, 2017).

1.2 Problem Statement

The aerostat is designed to have a low drag hull envelope shape and net static lift due to buoyancy to reduce the blow-by. The net static lift is obtained by making the aerostat hull volume bigger that will contain more LTA gas resulting in the increase in cost. It also produces consistent tension force on tether and ground handling problems.

1.3 Research Objectives

This study has followings objectives:

- i. To optimize design parameters of a tactical low altitude tethered aerostat that can uplift a payload mass of 5 to 50 kg.
- ii. To analyze the dynamical stability of the tethered aerostat in multiple wind scenarios.

1.4 Research Scope

This research presents the design and optimization of a tactical TAS with a communication equipment payload at low altitude. The TAS is composed of different subsystems that include winch, tether, payload and the aerostat. The primary focus of the study is on the aerostat, consists of a hull that contains LTA gas and fins for stability. For low altitudes, the variation of air pressure from the launch point is not

significant. Therefore, the design will not include a ballonnet that regulates the internal pressure.

This research thesis is aimed to obtain a tactical aerostat with a low drag coefficient hull shape that will have an increase in the net lift force by utilizing the aerostat fins. The fins will generate higher levels of the aerodynamic lift which produced when acted upon the wind, causing an increase in the system lift to drag ratio and will function both for reducing the blow-by and providing directional stability. The resulting configuration of the TAS will have a lower hull volume, saving a fabrication cost and can be easily deployed through a minimum workforce that will allow it to be used as an emergency respondent system to restore communication, aftermath a natural disaster.

1.5 Thesis Outline

This thesis is divided into five chapters that include an introduction, literature review, methodology, result and discussion, and conclusion. Chapter 1 describes general overview of the study done in this thesis. It explains the needs of tethered aerostats for communication provision to disaster-affected areas. It also provides a general introduction to the tethered aerostats, objectives and scope of the research.

In Chapter 2 literature review of tethered aerostats is laid down. An introduction to a tethered aerostat system is given by discussing its subsystems. The categorization of the aerostats into tactical, operational and strategic classes is also presented. The design process and design parameters for the aerostat are discussed, referring to the published work. A detailed literature review on the optimization of the aerostat design is laid down along with the research gap. The dynamic stability analysis research works done in previous studies are also summarized.

Chapter 3 contains the details related to the conceptual design of the aerostat. The sizing, aerostatics, aerodynamics and stability and the steps involved in the design of the aerostat are laid down. The steps involved in developing the design algorithm using MATLAB® is explained. The sensitivity analysis using the design code and design parameters are presented as well. Optimization algorithms that are used to obtain design variable values for optimized configuration are explained. Finally, the development of the 3DOF model for the aerostat dynamic stability analysis is presented.

Chapter 4 presents the results of the aerostat design in detail. The baseline configuration obtained using the design code is presented. The results of the sensitivity of the design variables on the aerostat design are discussed. The results of the optimization of the configuration using three different algorithms are presented, and the optimized configuration is compared with the baseline configuration. The operation of the design app for the aerostat is introduced as well. Finally, the results of the dynamical stability analysis for the optimized configuration for multiple wind scenarios are laid down.

Chapter 5 contains a summary of the research done in this research thesis and future work to be done for improvement. The contribution of this research thesis and the research publications are listed at the end of the chapter.

CHAPTER 2

LITERATURE REVIEW

This chapter presents the literature review of this research thesis. It begins with introducing the TAS and its sub-systems. The categorization of aerostat based on its size, altitude and endurance are also presented. The previous studies related to the design process, optimization and dynamical analysis are discussed, and the research gap is identified.

2.1 Introduction to Tethered Aerostat Systems

Aerostats are LTA systems that utilize LTA gas to keep airborne and it is connected to the ground station via a tether. Currently, TAS application is known for its economical solution for different applications due to their low power consumption. Ideally, it requires less or no power to float in the air as the LTA gas inside its envelope provides the buoyancy force for this purpose, while the tether maintains its position. The only power required for their operation is for the payload and onboard electronics. Alternatively, the power can be supplied through solar power, onboard batteries, or ground generator via a live tether cable.

2.2 Subsystems of TAS

The TAS's subsystems includes the aerostat, payload, tether, winch and mooring station as depicted in Figure 2.1 (Tenenbaum, 2016; Bajoria *et al.*, 2017).

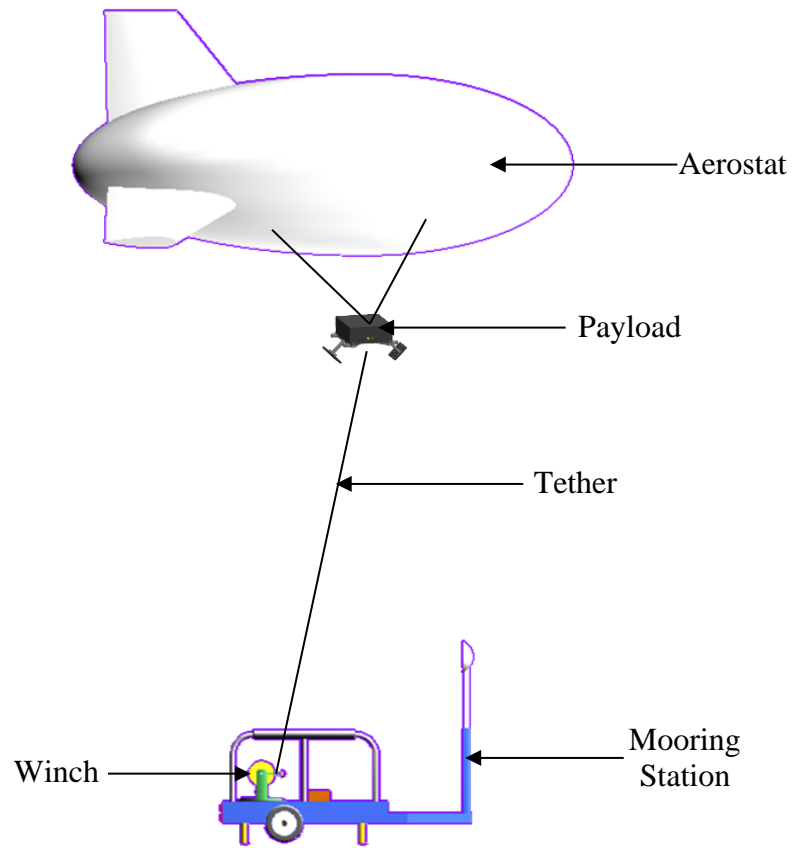


Figure 2.1 Aerostat Subsystems

2.2.1 Aerostat

The Aerostat itself is a non-rigid structure that holds the LTA gas. The amount of LTA gas provides the required amount of the buoyancy force required. The constructing materials consists of a laminated multi-layer fibre-reinforced composite (Li *et al.*, 2019) provides leak proofing, strength and environmental protection. The aerostat hull envelope can be designed in many shapes depending upon the application the aerostat. Among others, spherical and streamlined envelope shapes appear to be the most popular for aerostat hull (Coulombe-Pontbriand, 2005).

2.2.1(a) Aerostat Hull Shapes

The spherical aerostat has numerous advantages that include ease of fabrication, low cost and compact (Miller and Nahon, 2005; Pant *et al.*, 2011). They do not require any preferred orientation to the wind direction due to symmetric shape. The spherical shape has the lowest possible surface-area-to-volume ratio, thereby making spherical aerostats lightweight. Despite the prominent advantages, the spherical aerostat has higher drag coefficient C_D that causes them higher blow-by due to wind. Experimental studies conducted by Coulombe-Pontbriand and Nahon (2009) shows that a tethered sphere in a natural wind field has a drag coefficient of 0.56. Some design modifications like net curtains are used to reduce the blow-by of the spherical aerostat, as shown in Figure 2.2. Net curtain generates dynamic lift from the wind force that helps in reducing the blow-by of the aerostat.



Figure 2.2 Skystar 220 Spherical Aerostat (RT, no date)

Helikites, a hybrid shape aerostat designed by Sandy Allsopp, also has a spherical hull shape, as shown in Figure 2.3. The kite structure attached to the hull reduces the blow-by by generating aerodynamic lift from the wind. The keel is placed perpendicular to the kite, and it aligns the Helikite with the ambient wind direction. The aerodynamic lift generated by the kite also reduces the amount of static lift

required, eventually the size of the balloon can be reduced, making the system compact (Rogers, 2001).

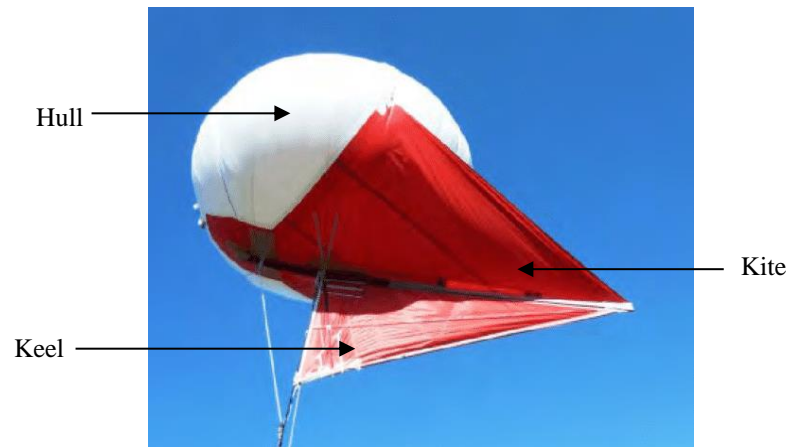


Figure 2.3 Helikite (Allsopp Helikites Ltd, no date)

Despite the advantages of spherical aerostats, the most popular shape for the hull envelope consists of an elongated shape like an airfoil known as streamlined or aerodynamic shape due to lower values of C_D of around 0.02. Figure 2.4 shows streamlined aerostat whose shape are similar to those used in the airships, aircrafts, and submarines that move in a fluid (Gertler, 1950). The low C_D of streamlined aerostats makes them capable of operating in high wind conditions as they have low blow-by. Their surface area is greater as compared with the spherical aerostats, making them relatively heavier. The tail fins present at the rear end provide a restoring moment to stabilize the attitude of the aerostat and align the aerostat with the wind (Bajoria *et al.*, 2017). The fins are mostly designed as a part of the envelope that are filled with LTA gas for their structural strength (Ram and Pant, 2010). The streamlined aerostat that is in service have uncontrolled fins, however, (De Azevedo, Góes and Azinheira, 2017) and (Howard, 2007) has demonstrated the use of controllable fins that improves the performance in turbulent winds.



Figure 2.4 Streamlined Shape Aerostat (TCOM, 2018)

2.2.1(b) Aerostat Hull Shape Comparison

Table 2.1 provides a comparison between the different hull shapes in terms of operating altitude, wind conditions it can sustain, launch conditions, payload limit and the drag coefficient.

Table 2.1 Aerostat hull shapes comparison (Mahmood, Ismail and Suhadis, 2020)

Properties	Spherical	Helikite	Streamlined
Operating Altitude	~1 km	~2 km	~ 5 km
Wind Conditions	10 m/s	25 m/s	50 m/s
All-Weather Operation	Limited	Yes	Yes
Payload Limit	~50 kg	<30 kg	~3,200 kg
Drag Coefficient	0.15~0.4	0.15~0.4	0.03

The comparison between the blow-by performance for a different type of aerostats is presented in Figure 2.5 that is obtained by using the parameters listed in Table 2.2.

Table 2.2 Hull Shape Parameters for calculating Blow-by

Sr.	Parameter	Helikite	Spherical	Streamlined
1.	Volume	100 m ³	100 m ³	100 m ³
2.	Hull Length	6.2 m	5.76 m	11.2 m
3.	Hull Width	5 m	5.76 m	4.1 m
4.	Altitude	300 m	300 m	300 m
5.	Buoyancy Force	100 kg (981 N)	100 kg (981 N)	100 kg (981 N)
6.	Mass Breakdown	Helium = 16.9 kg Hull = 13.72 kg Kite = 11.38 kg Tether = 6 kg Total = 48 kg	Helium = 16.9 kg Hull = 13.54 kg Tether = 6 kg Total = 36.45 kg	Helium = 16.9 kg Hull = 15.57 kg Fins = 7.8 kg Misc = 4.7 kg Tether = 6 kg Total = 50.92 kg
7.	Free Lift	52 kg	63.55 kg	47 kg
8.	Dynamic Lift at 15 m/s Wind Speed	48 kg	Nil	Nil
9.	Drag Coefficient	0.2	0.2	0.03
10.	Max Wind Speed	15 m/s	15 m/s	15 m/s

The calculations are done by considering the following parameters:

- Helikite Aerostar system is taken as reference, and its parameters are obtained from the manufacturer website (Allsopp Helikites Ltd, no date).
- The volume for all three aerostat shapes are equal.
- Streamlined Aerostat has NPL shape with 2.7 fineness ratio, and the mass of fins are taken as a ratio of total mass from the work of Gawande *et al.*, (2007).
- The lift generated by streamlined aerostat is ignored.
- The hull material is the same for all three aerostat shapes.
- The tether sagging is ignored for these calculations.

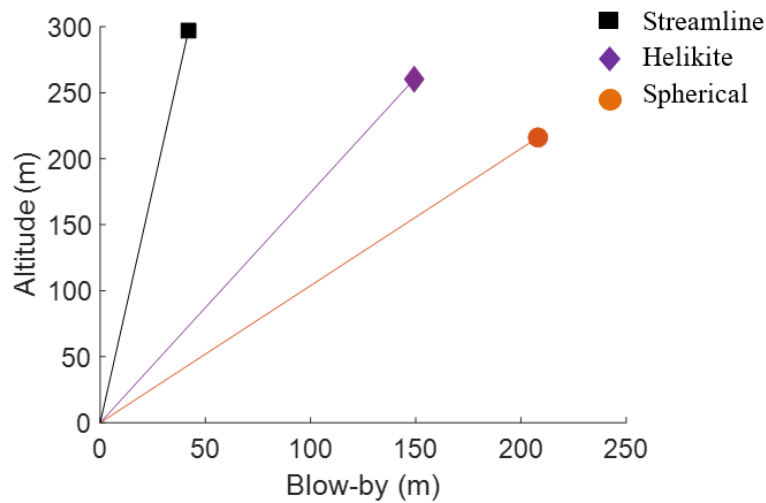


Figure 2.5 Blow-by comparison of different hull shapes

The results show that the streamlined aerostat has the lowest blow-by due to its lower drag coefficient. The Helikite has lower blow-by than spherical due to dynamic lift generation despite having an ellipsoidal hull that has a higher drag coefficient. This shows that streamlined aerostat can be further improved by incorporating dynamic lifting capability like Helikite.

2.2.1(c) Ballonet

Aerostat hull consists of a non-rigid structure that is made up of composite fabric material. The internal overpressure of the LTA gas provides strength to maintain its shape. However, the variation in air density with altitude requires the hull internal pressure to be regulated during its ascent and descent phase of flight. The change in air density also occurs with variation in weather that needs to be adjusted (Kumar, Sati and Ghosh, 2016). For this purpose, a ballonet as shown in Figure 2.6 is added to the hull of the aerostats that are to operate at altitude levels that have a significant change in the air density. A pressure system that consists of valves, pressure sensors and blowers maintains the ballonet pressure (Ashford and TCOM, 1982). However, for

small-sized aerostats, whose operational height is lower, the internal pressure of the aerostat is maintained by the used of elastic cords and called passive ballonet. A design study by Bajoria *et al.* (2017) mentions that if the operational height of aerostat is less than 500 m, it can be flown without a ballonet as there is less variation in the air pressure.

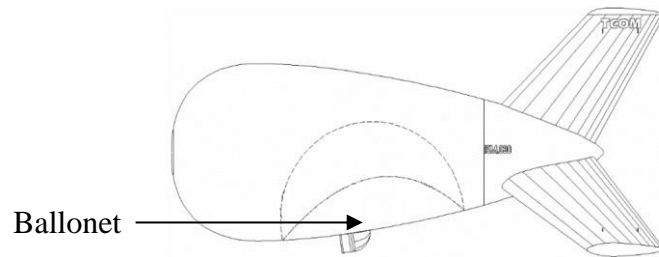


Figure 2.6 Ballonet (TCOM, 2018)

2.2.1(d) Aerostat Hull Material

The material that is used to build the envelope should have the following characteristics (Dasaradhan *et al.*, 2018).

- The material must have low gas permeability to avoid loss of gas from the hull.
- The material must be lightweight to decrease the weight of the structure of the aerostat to increase payload capacity.
- The material should have sufficient strength to withstand different stresses that acts on the hull during operation.
- The material should have high tear resistance because it can cause catastrophic failures even due to small tears during handling.
- The material should be resistant to ultraviolet radiations, humidity, heavy winds and extreme weather conditions.

The aerostat hull envelope material is formed as a flexible laminate constructed from different layers, as shown in Figure 2.7. The innermost layer is the strength layer

that is the load-bearing layer and is made up of woven synthetic fibres. The strength layer has gaps that cannot resist the leakage of gas; therefore, the gas barrier layer composed of polymeric materials are used as laminated thin films or coatings. The most used materials for gas barrier layers are polyvinyl fluoride, neoprene and polyurethane. The exterior layer is an environmental protection layer that helps the degradation of material from ultraviolet rays. Polyurethane material can also protect from ultraviolet rays. High reflectivity metals such as silver and aluminum can also be used to coat that can reflect the ultraviolet rays of the sun. The different layers of the laminate material are bonded by chemical or mechanical means (Dasaradhan *et al.*, 2018).

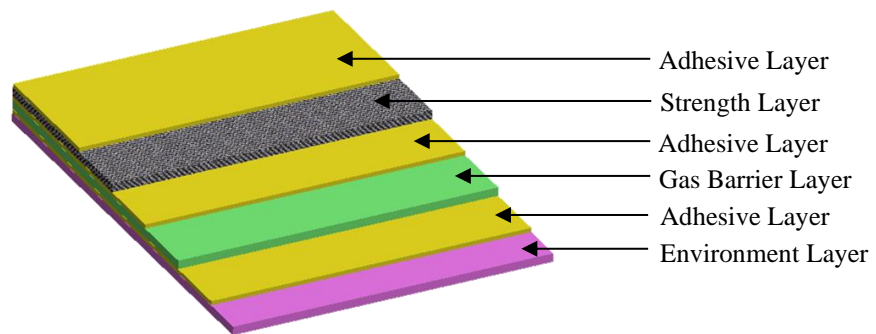


Figure 2.7 Aerostat Hull Material Layers

2.2.2 Payload

The payload contains electronics and other mission equipment that is to be airborne at a specified altitude. For surveillance operations, the (EO/IR) payload is carried that consists of visual and infrared sensors to provide day and night surveillance of an area of a target. For the application of Aerostat of providing communication from the sky, the communication equipment that it uses as the payload is composed of Antennas and Remote Radio Head (RRH) as shown in Figure 2.8.



EO/IR Payload
(FLIR Systems, 2019)



Comms Payload
(Chandrasekharan *et al.*, 2016)

Figure 2.8 Aerostat Payloads

2.2.3 Tether

The tether is a strong rope that connects the aerostat to the ground and maintains its position. The aerostat envelope is connected to a series of ropes known as confluence line that converge at the confluence point to which the tether is attached (Kanoria and Pant, 2012). Some aerostats use a single tether that also provides electric power to the aerostat electronics from the ground called a live tether. At the same time, others have separate tethers for position control and power transmission. Linden Photonics Micro Tether made to be used for airborne drones and aerostats is shown in Figure 2.9.

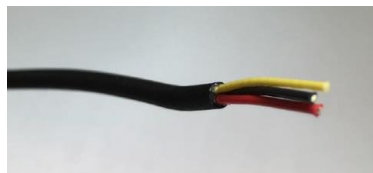


Figure 2.9 Live Tether for Aerostat (Linden Photonics, 2020)

2.2.4 Winch

The tether is wound on the winch that has a mechanism to control the inhaul and outhaul of a tether during ascent and descent phase and during a flight of the

aerostat as shown in Figure 2.10. The winch is attached to a base structure that can revolve 360 degrees and a motor is connected to the winch through a driver mechanism. The proper winding of the tether on the winch is obtained by a winder mechanism that operates on rack and pinion mechanism. The DC Electric motors are used for synthetic tethers that can provide extension and retrieval speeds around 60 feet per minutes. Hydraulic motors are used for live tether that contains copper wiring and fiber optic connectivity to the payload. To save the tether from breaking the central drum is sized bigger that does not violate the bending radius limit of tether. The power of hydraulic motors is determined after calculating the tether pull and release speeds.

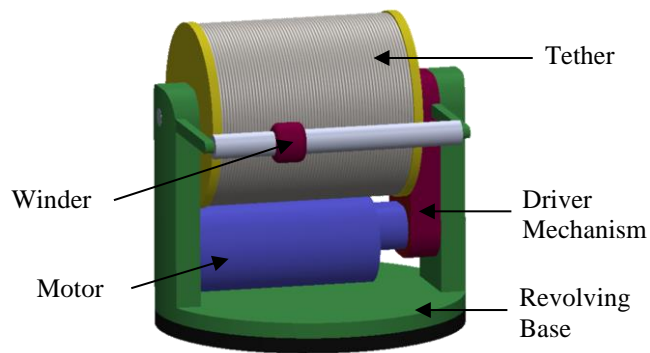


Figure 2.10 TAS Winch System



Figure 2.11 Winch (Thern, 2019)

2.2.5 Mooring Station

The ground preparation and deployment of the aerostat is done from the mooring station. This station is designed to hold the aerostat at the ground before launch and during routine maintenance of the aerostat. For small aerostats it is a mobile unit that can be transported via a vehicle to the required deployment site as shown in Figure 2.12. For huge aerostats, mooring station can be a permanent installation as shown in Figure 2.13, while (TCOM, 2018).



Figure 2.12 Mooring Station of Smaller Aerostat (SkySentry, no date)



Figure 2.13 Mooring Station of Larger Aerostats (SAVER, 2013)

Figure 2.14 shows an illustration of a mooring station with labelled parts. It has a docking mast that holds the aerostat from the nose latch when it is inflated. The aerostat rests on the support table, and it provides access to the of the aerostat. The jacks are provided at the base of the mooring stations that stabilizes the platform during operation of the aerostat. The winch and electric generator are mounted on the mooring station platform.

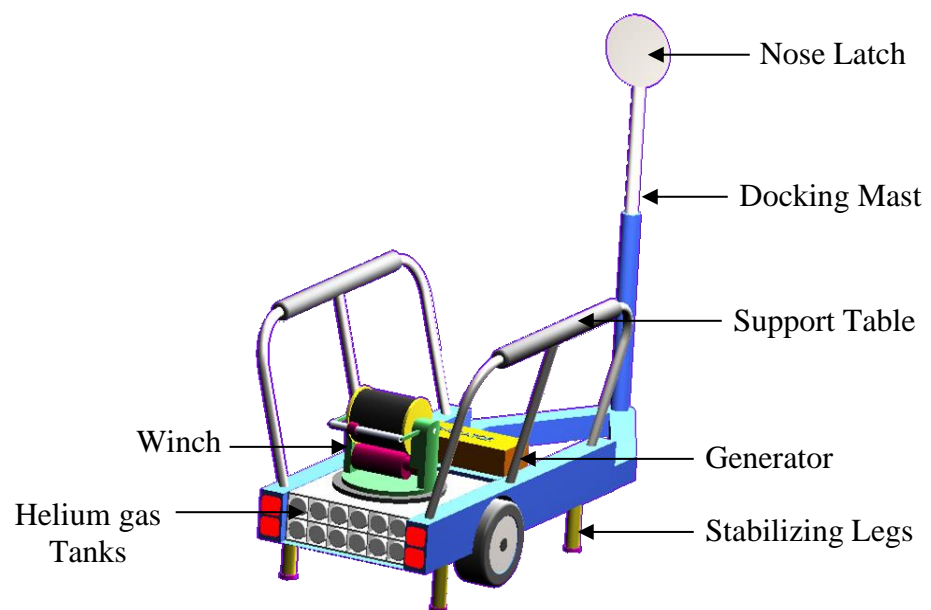


Figure 2.14 Mobile Mooring Station

2.3 TAS Categorization

The aerostat can be categorized into three classes based upon the payload carrying capacity, operational altitude and size. Table 2.3 contains information regarding categorization of different aerostats that are in service along with their properties. The aerostat designed in this research thesis falls in tactical aerostat category.

Table 2.3 Tactical, Operational and Strategic Class Aerostats (SAVER, 2013)

Sr.	Manufacturer	Model No.	Length (m)	Diameter (m)	Maximum Payload (kg)	Altitude (m)
TACTICAL CLASS AEROSTAT						
1.	Raven Aerostat	TIF-1600	9.6	3.3	16	0 - 610
2.	TCOM	12M	12	-	27	0 - 300
	TCOM	17M	17	-	90	0 - 300
3.	Sky Crow	TA	10.3	-	9	0 - 305
4.	Airstar	White	4.4	3.4	5	0 - 200
	Aerospace	Hawk				
5.	Top Vision	T.A.S	9.1	2.9	4	0 - 150
6.	Sky Sentry	HEA-150			25	0 – 300 m
OPERATIONAL CLASS AEROSTAT						
1.	TCOM	22M	22	-	190	900
2.	TCOM	28M	28	-	570	900
3.	Sky Sentry	HEA 3000		-	450	1500
4.	RAVEN	TIF-25K	23.2	7.6	227	900
5.	Aeroscraft	AEROS 3200	39		300	1500
STRATEGIC CLASS AEROSTAT						
1.	TCOM	71M	71	-	1600	0 - 4600
2.	TCOM	74M	74	-	3200	0 - 3000

2.3.1 Tactical Aerostats

Tactical class aerostats are readily deployable highly portable systems. These systems carry a payload for land surveillance applications. Their payload carrying capacity is up to 30 kg that can be lifted to a height of 300 m above ground level. The size of the aerostat is around 170 m³ and flight endurance is 5 to 7 days. They can operate and survive up to 20 m/s wind conditions (TCOM, 2018).

2.3.2 Operational Aerostat

These aerostats are medium-sized aerostats that have a volume of the range 800 to 1600 m³. They can lift a payload of 130 kg to 360 kg to a height of 1000 m to 1500 m. The payload carried by these aerostats includes radar, SIGINT and COMMS relay that are used for surveillance applications (TCOM, 2018). They can stay up in the air from 7 days to 4 weeks on helium gas addition and can operate up to 26 m/s wind speeds (Krausman and Petersen, 2013).

2.3.3 Strategic Aerostats

The strategic aerostats are the largest size systems that can operate at an altitude of 3000 m to 5500 m above sea level. They have payload carrying capacity of 1500 kg to 3000 kg. The payload includes long-range radars, active and passive communications equipment. They can be deployed continuously for 30 days and can survive in a wind speed of 36 m/s (TCOM, 2018).

2.4 TAS Design Process

The design process of a TAS involves various disciplines that include structure, aerodynamics, aerostatics and stability analysis. The design process followed by previous studies indicate that it is carried out iteratively (Raina, Gawale and Pant, 2008; Pant and Kapoor, 2013; Kumar, Sati and Ghosh, 2016; Bajoria *et al.*, 2017). The design cycle is continued until the required payload capacity is obtained. The design process chart is shown in Figure 2.15.

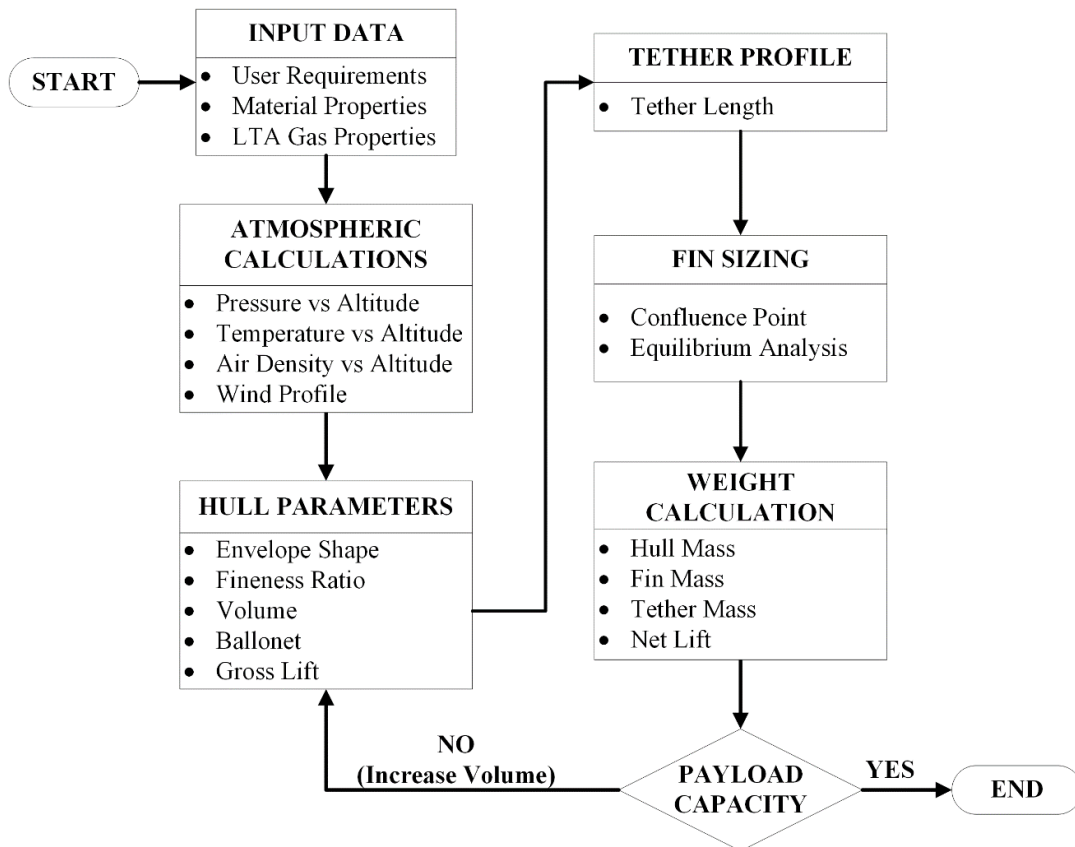


Figure 2.15 Aerostat Design Process

2.4.1 Input Data

2.4.1(a) Payload Specifications

The user requirements specify the operational requirements, location specification and power requirement for the payload (Gawande *et al.*, 2007; Bajoria *et al.*, 2017). The detailed list of the user requirements is given in Table 2.4.

Table 2.4 User Requirement

Operational Requirements	<ul style="list-style-type: none"> i. Payload mass ii. Payload size iii. Floating Altitude iv. Blow-by v. Permissible reduction in altitude
Location Specification	<ul style="list-style-type: none"> i. Base station altitude ii. Wind Variation iii. Temperature at launch site

Table 2.4 Continued

Power Requirement	<ul style="list-style-type: none"> i. Onboard power source ii. Power requirement from ground to onboard via tether
--------------------------	--

2.4.1(b) Material Properties

The material properties include the fabric grams per square meter (GSM) value that will be used to construct the aerostat hull and fins (Gawande *et al.*, 2007). The GSM of fabric is used to calculate the mass of the aerostat structure. The tether material density is available in grams per meter and is used in the estimation of tether mass (Linden Photonics, 2020).

2.4.1(c) LTA Gas Properties

The LTA gas lifting force, density and purity are the properties required in the design process. Helium and Hydrogen are the two candidate gases, and the latter is the most used due to its inflammability and availability. Helium is available at a high purity level of about 98%. Its price is higher than other gases, but its ease of operation makes it the best candidate for LTA vehicles (Ganesh and Sai Kumar, 2018). Table 2.5 shows the properties of Helium and Hydrogen.

Table 2.5 LTA gas properties

Gas	Density	Lifting Force	Properties
Hydrogen	0.085 kg/m ³	11.2 N/m ³	Inflammable, relatively cheap
Helium	0.169 kg/m ³	10.2 N/m ³	Inert, relatively expensive

2.4.2 Atmospheric Calculations

The atmospheric calculations to determine the air pressure, density and temperature involve generating a profile of variation of these parameters with altitude.

Bajoria *et al.* (2017) have done the calculations of the pressure, density and temperature based on ISA (International Standard Atmosphere). The off standard temperature values of the launch site are used to adjust the values of these parameters.

2.4.3 Hull Parameters

2.4.3(a) Envelope Shape Selection

The hull envelope shape is a low drag shape that is optimized for multi-disciplines. Some standard low drag hull shapes to be used as aerostat hull envelopes are available in literature like are NPL, GNVR, Wang and ZHIYUAN-1 shown in Figure 2.16. NPL shape is designed by National Physics Laboratory and consists of two ellipsoids of revolution, which meet at the location of maximum diameter (Khoury and Gillett, 1999). GNVR shape, named after G. N. V. Rao of the Indian Institute of Science, who developed it. The profile of the GNVR shape is a combination of an ellipse, circle, and parabola (Ram and Pant, 2010). Wang shape has been developed by Multidisciplinary optimization through a genetic algorithm (Wang *et al.*, 2009). Zhiyuan-1 is an unmanned blimp developed by Vantage Airship and Shanghai Jiao Tong University (Wang and Shan, 2006; Wang *et al.*, 2010).

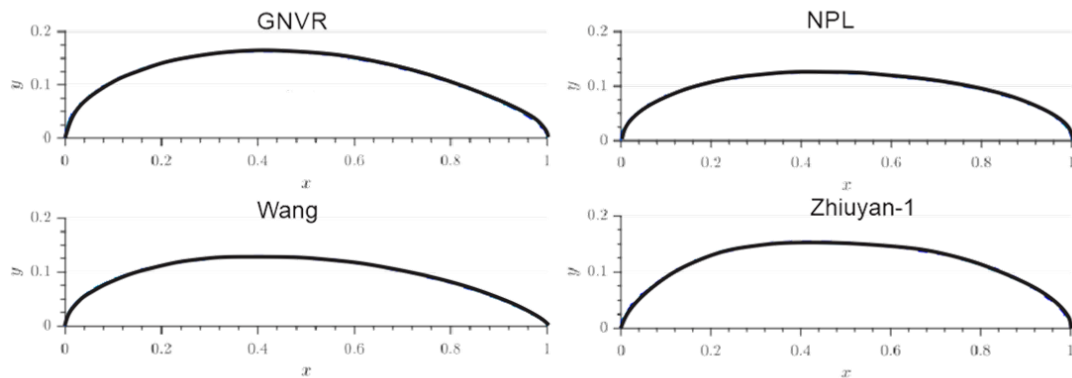


Figure 2.16 Standard Streamlined Shapes (Alam and Pant, 2017)